Hydrogen Bond versus Anti-Hydrogen Bond: A Comparative Analysis Based on the Electron Density Topology

E. Cubero,[†] M. Orozco,*[,†] P. Hobza,[‡] and F. J. Luque*[,§]

Departament de Bioquímica i Biologia Molecular, Facultat de Química, Universitat de Barcelona, Martí i Franqués 1, 08028 Barcelona, Spain, J. Heyrovsky Institute of Physical Chemistry, Academy of Sciences of the Czech Republic, 182 23 Prague 8, Czech Republic, and Departament de Fisicoquímica, Facultat de Farmàcia, Universitat de Barcelona, Av. Diagonal s/n, 08028 Barcelona, Spain

Received: January 22, 1999; In Final Form: April 14, 1999

The theory of atoms in molecules is used to examine the nature of anti-hydrogen bond (anti-H bond) interaction. Contrary to what is found in normal hydrogen bond (H bond) complexes, which are characterized by lengthening of the X−H bond and a red shift of its stretching frequency, the anti-H bond leads to a shortening of the X−H bond length and a blue shift of its vibrational frequency. The topological properties of the electron density have been determined for a series of C−H···π complexes, which exhibit either anti-H bond or normal H bond character, as well as for the complexes C_6H_5F···$HCCl_3$ and C_6H_6···HF, which are representative cases of anti- and normal H bonds. Inspection of the set of topological criteria utilized to characterize conventional H bonds shows no relevant difference in the two classes of H···π complexes. Analysis of the results suggests that the specific features of the anti-H bond originates from the redistribution of electron density in the C−H bond induced upon complexation, which in turn evidences the different response − dispersion versus electrostatic− of the interacting monomer for stabilizing the complex.

Introduction

The hydrogen bond (H bond) is a key interaction in molecular recognition.[1,2] From an energetic point of view, a H bond typically contributes a few kilocalories per mole to the stabilization of H-bonded complexes, even though it can be as large as −50 kcal/mol in complexes such as $(FHF)^-$.[3] The H bond presents an interesting set of properties such as cooperativity and directionality, which are relevant for determining a wide range of structural properties, like the aggregation states of water[4] and the stability of biomolecules.[5] Indeed, the distribution of H bond donors and acceptors has a functional role in modulating the specificity of recognition and binding in chemical and biological systems.[2] This feature has been exploited, for instance, to design new agents in the context of antigen and antisense therapies.[6]

Conventional H bond interactions (X−H···Y) involve two electron-withdrawing atoms (X,Y are usually nitrogen, oxygen, or fluorine), one being attached to a hydrogen atom and the other bearing lone electron pairs. These complexes are characterized by a lengthening of the donor X−H bond and by a concomitant red shift in the X−H stretching frequency. Nevertheless, recent studies have shown that such a concept of hydrogen bonding is not complete and can be extended to other complexes, like those involving the interactions with π charge distributions (Y: π-electron system)[7] or with carbon atoms acting as hydrogen donors (X: carbon).[8] Indeed, a new type of H bond, called a dihydrogen bond, has been introduced to explain certain interactions where a hydrogen is directly donated to another hydrogen (X−H···H−Y), the latter being negatively charged.[9] These interactions have been described in systems containing transition metals and boron, which can accommodate the hydridic hydrogen.[10]

Recently, Hobza et al.[11] have suggested the existence of a new type of bonding, termed anti-hydrogen bond (anti-H bond), which has been identified in the T-shape structure of the benzene dimer and other benzene complexes interacting with carbon proton donors. In contrast to the features observed in conventional H bonds, the anti-H bond is characterized by a shortening of the C−H bond and by a blue shift of the C−H stretching frequency. Stabilization in these complexes originates dominantly in the London dispersion energy and no (or very small) stabilization is found at the Hartree−Fock level.[11] Dispersion attraction is proportional to the higher power of the reciprocal distance of the centers of mass of both subsystems. To minimize the distance and thus optimize the dispersion attraction, it is advantageous to compress the C−H bond of the proton donor. Forces causing shortening of the C−H bond are responsible for making the C−H stretching potential deeper and narrower, and thus allow for a blue shift of the corresponding stretching frequency. Recently, the predicted anti-H bond nature of the complex between chloroform and fluorobenzene has been confirmed experimentally.[12]

To gain insight into the nature of anti-H bond, this study reports a comparative analysis of the electron density topology in complexes corresponding to normal H bonds and anti-H bonds for a series of C−H···π complexes. The theory of "atoms in molecules" (AIM)[13] offers a rigorous way of partitioning any system into its atomic fragments considering the gradient vector field of its electron density. By means of a topological analysis of the electron density, features such as bond critical points and paths of maximum electron density can be utilized to draw a

* To whom correspondence should be sent.
[†] Departament de Bioquímica i Biologia Molecular.
[‡] J. Heyrovsky Institute of Physical Chemistry.
[§] Departament de Fisicoquímica.

10.1021/jp990258f CCC: $18.00
Published on Web 07/27/1999

TABLE 1: Length (bl; Å) and Harmonic Stretching Frequency (ν; cm^{-1}) of the C−H Bond in the Isolated Monomer (m) and in the Dimer (d), and the Interaction Energy (kcal/mol) of the Complex

compound	bl(m)	bl(d)	Δbl	ν(m)	ν(d)	Δν	ΔE^a
CH_4	1.0855	1.0846	−0.0009	3278	3293	+15	−0.4 (−1.5)
$HCCl_3$	1.0829	1.0806	−0.0023	3256	3307	+51	−3.2 (−6.5)
C_6H_6	1.0827	1.0793	−0.0034	3283	3325	+42	−1.2 (−3.5)
HCCH	1.0625	1.0633	0.0008	3588	3586	−2	−1.6 (−3.7)
HCN	1.0652	1.0667	0.0015	3531	3515	−16	−3.2 (−5.4)
HF	0.9211	0.9239	0.0028	4194	4153	−41	−2.8 (−5.3)
$HCCl_3$[b]	1.0829	1.0802	−0.0027	3256	3309	+53	−2.5 (−5.8)

[a] The interaction energy estimated without correction for the basis set superposition error and geometry distortion of the monomers upon complexation is given in parentheses. [b] Complex of chloroform with fluorobenzene.

molecular graph (i.e., the network of bond paths that connects linked atoms). In particular, an H bond is evidenced in the charge density by a bond path linking the proton and the acceptor atom. AIM has been successfully used to characterize H bonds in a variety of molecular complexes.[7a,7e,8c,9b,14] Several studies have also shown a clear relationship between the topological properties of the charge density in H-bonded complexes with both the interaction energy and the internuclear distance of the complexes.[7e,15] Therefore, AIM seems well suited to examine the very nature of the anti-H bond in molecular clusters.

Methods

To examine the electron density topological properties in H bonds and anti-H bonds, the benzene complexes with CH_4, $CHCl_3$, C_6H_6, and HCN were considered. These complexes were chosen following Hobza et al.,[11] who used them to discuss the C−H···π anti-H bonds for the proton donors CH_4, $CHCl_3$, and C_6H_6, which exhibited changes (shortening of the C−H bond and blue shift in the stretching frequency) opposite to those expected for a normal H bond, as was found in the complex of benzene with HCN (lengthening of the C−H bond and red shift in the stretching frequency). In addition, we considered the interaction of benzene with HCCH and HF. Because HCCH can be viewed as an apolar isoster of HCN, inspection of the topological properties can be of interest for a comparative analysis. On the other hand, inclusion of the complex between benzene and HF is useful as a reference model because this complex is expected to behave as a prototypical normal H bond. Finally, the analysis was extended to the H bond interaction in the complex of chloroform with fluorobenzene because the blue shift in the C−H stretching frequency predicted by theory has been confirmed experimentally.[12]

The geometries of complexes and isolated monomers were optimized at the second-order Møller−Plesset level[16] using the 6-31G(d,p)[17] basis set and the frozen core approximation. No symmetry constraint was imposed in the optimization. In the starting geometry, the complexes were built up with the donor C−H group oriented along the line normal to the plane of benzene passing through the center of the ring. For the complex of chloroform with fluorobenzene, we used as starting geometry the MP2/6-31G(d) optimized one reported by Hobza in ref 12. The minimum energy nature of the optimized structures was verified from vibrational frequency analysis. With exception of the benzene complexes with methane and hydrogen fluoride, the optimized geometries present the donor C−H group pointing toward the center of the benzene ring. In the C_6H_6···HCH_3 and C_6H_6···HF complexes, the C−H and F−H bonds are pointing toward a carbon atom of the ring, and the optimized geometry has a C_s symmetry. To compare the topological properties of the electron density, additional energy minimization calculations were performed for these two complexes imposing the C−H and F−H bonds to be oriented along the normal line passing through the center of the benzene ring. Even though the final structures presented nonzero negative frequencies, they were used in the analysis because they exhibit a common topological pattern with the other benzene complexes (vide infra). However, comparison is also made of the topological properties of the C_s-optimized structures. The interaction energies were corrected for the basis set superposition error using the counterpoise correction.[18] The C−H stretching frequency shifts induced upon complexation were determined within the harmonic approximation because the introduction of anharmonicity does not substantially modify the results.[11] All these calculations were performed with Gaussian 94.[19] The topological analysis and the integration of selected atomic properties (vide infra) was performed with the programs EXTREME and PROAIM.[20]

Results and Discussion

Table 1 reports the lengths and harmonic stretching frequencies of the C−H bond in the monomer and the dimer, and the interaction energy of the dimer, for the benzene complexes with CH_4, $CHCl_3$, C_6H_6, HCN, HCCH, and HF, as well as of chloroform with fluorobenzene. In all cases, the C−H (F−H) bond is pointing toward the center of the ring. Upon complexation, the C−H bond length decreases for CH_4 (−0.0010 Å), $CHCl_3$ (−0.0023 Å; −0.0027 Å for the complex with fluorobenzene), and C_6H_6 (−0.0034 Å),[11] whereas the reverse effect occurs in HCN (+0.0153 Å) and HCCH (+0.0008 Å). This latter trend is also found in the complex with HF, where the H−F bond length increases 0.0028 Å. The lengthening/shortening of the C−H bond upon complexation is also reflected in the change of the corresponding stretching frequency. Thus, whereas benzene complexation leads to a blue shift in the range +15 to +51 cm^{-1} for CH_4, $CHCl_3$, and C_6H_6, the C−H frequency is red shifted very slightly in HCCH (−2 cm^{-1}) and more remarkably in HCN (−16 cm^{-1}), as it is also found in the complex with HF, where the H−F stretching frequency is red shifted by 41 cm^{-1}. In summary, in contrast to the behavior exhibited by conventional complexes, such as C_6H_6···HCN and C_6H_6···HF, the reverse features found for other complexes provides the basis for the concept of the anti-H bond.[11]

In the true minimum energy structures of the complexes of benzene with methane and hydrogen fluoride (see *Methods*) the C−H and F−H bonds are pointing toward a carbon atom of the ring (the C−H or F−H axis forms an angle of ∼15° with the line normal to the benzene passing through the center of the ring). The optimized geometry for C_6H_6···HF differs from the minimum energy structures reported in previous studies, where a C_{6v} symmetry was found at the RHF/6-31G(d) level,[7a] and where the HF molecule points toward the middle point of one of the C−C bonds at the MP2/6-311++G(d,p) level.[14c] The energy of the MP2/6-31G(d,p) C_s structures differ only by a few hundredths of a kilocalorie/mole from the values reported

in Table 1, indicating that the energy surface is very flat and that the energy minimum is very shallow. For the purposes of our study, it is worth noting that in the C_s structures the C−H bond of methane is shortened by 0.0008 Å and the C−H stretching frequency is blue shifted by 13 cm^{-1}, whereas in contrast the H−F bond length is enlarged 0.0034 Å and a red shift of −59 cm^{-1} occurs in the vibrational frequency. Therefore, despite the different geometrical arrangement, the changes in bond length and stretching frequency observed in CH_4 and HF reflect the same differential trends already mentioned.

As noted before by Hobza et al.,[11] the stabilization in anti-H bond complexes originates dominantly in the London dispersion energy. Thus, decomposition of the interaction energies reported in Table 1 into their Hartree−Fock and MP2 components indicate that the former term is repulsive, varying from +0.7 kcal/mol for the complex of benzene with chloroform to +1.9 kcal/mol for that with benzene. In contrast, the Hartree−Fock component is stabilizing for the complexes of benzene with HCN and HF, where it contributes to around −1.9 kcal/mol to the total interaction energy.

In a series of studies, Popelier proposed a set of eight concerted effects occurring in the electron density that are indicative of hydrogen bonding.[8c,9b] These criteria comprise a set of local topological properties of the electron density and a set of integrated atomic properties related to the hydrogen atom involved in hydrogen bonding. With regard to the former set, the existence of a H bond implies (1) a correct topological pattern (a bond critical point and a bond path) for the proton donor and acceptor, proper values of (2) the electron density and (3) the laplacian of the electron density at the bond critical point, and finally (4) the mutual penetration of the hydrogen and acceptor atoms. The criteria concerning the integrated properties of the hydrogen atom involve (5) an increase of the net charge, (6) an energetic destabilization, (7) a decrease in the dipolar polarization, and finally (8) a decrease in the atomic volume. These properties have been determined for the different complexes considered in this study and are used to compare the AIM features in normal H bond and anti-H bonds.

(1) Topology of the Electron Density. The first necessary condition for the existence of an H bond is the identification of a (3,−1) bond critical point between the hydrogen atom and the acceptor associated with a bond path linking the corresponding atoms. In the C−H···benzene complexes considered here, the acceptor is the set of attractors formed by the carbon atoms in the benzene ring, and the formation of the H bond is reflected in the appearance of six (3,−1) critical points linking the hydrogen atom to each carbon atom[7a,e] (see Figure 1). In addition, a common feature to all the complexes is the occurrence of six (3,+1) ring critical points, which are placed between each pair of bond critical points. Finally, the C−H···π interaction is also characterized by the formation of a (3,+3) cage critical point. This topological pattern has also been described in complexes involving the interaction of cations with benzene.[7e]

The complex between chloroform and fluorobenzene is peculiar because just one bond critical bond exists, and the corresponding bond path connects the hydrogen atom in chloroform with the carbon in position *para* of fluorobenzene (see Figure 1). Indeed, the interaction is characterized by the appearance of a ring critical point near C1 and by a cage critical point over the center of the ring. It is worth noting that such topology satisfies the Poincaré−Hopf relationship, which relates the number and type of critical points that can coexist in a system with a finite number of nuclei. This topological

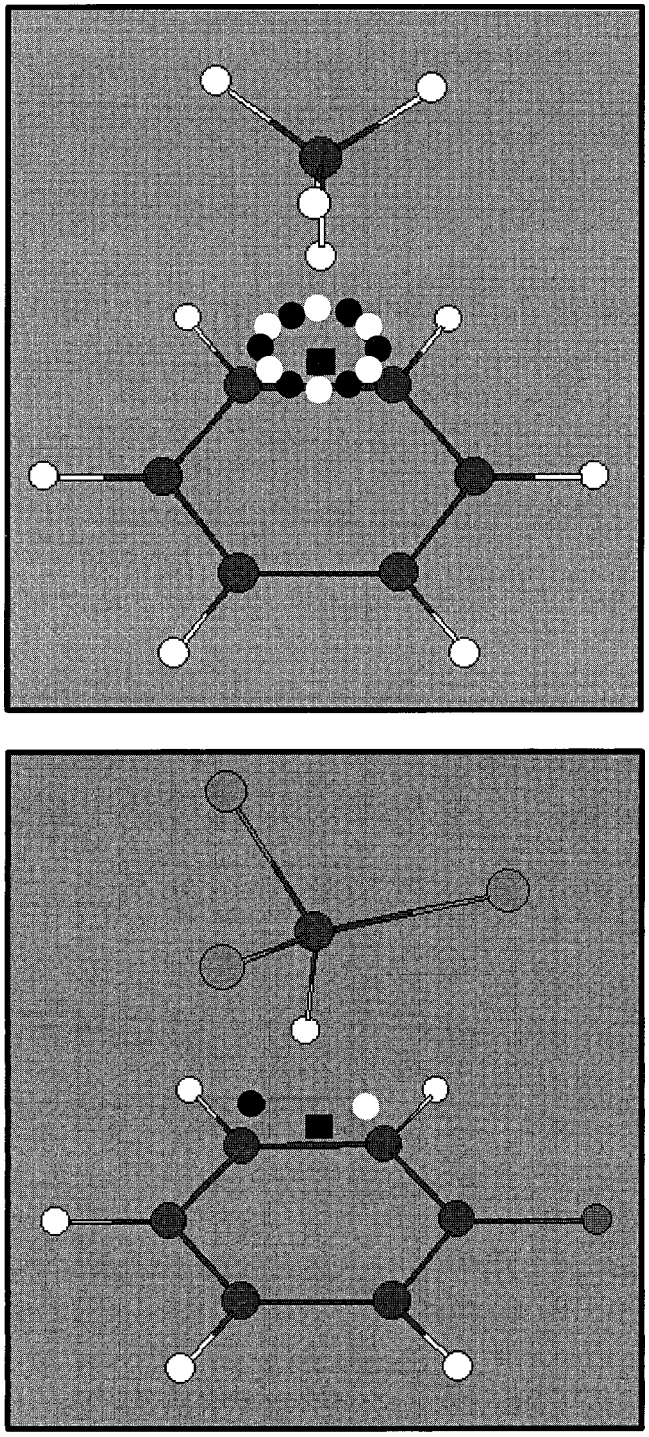

Figure 1. Representation of the dimer between benzene and methane (top) and fluorobenzene and chloroform (bottom) showing the location of the bond (dark circles), ring (white circles), and cage (square) critical points formed upon complexation.

arrangement has also been found in the complex of fluorobenzene with the Na^+ cation[7e] and reflects the influence of the fluorine atom on the electron density of the benzene ring. It suggests that the surface of the ring critical point extends from the C(*para*)-H bond path all around the ring back to the same bond path and, as a result, the topology of the electron density exhibits a cage critical point in the complex.[21]

The C_s structures for the benzene complexes with CH_4 and HF also exhibit a different pattern. In these cases, a single bond path links the hydrogen atom with the carbon atom to which the C−H (F−H) bond is pointing. In addition, a ring critical

TABLE 2: Topological Properties (au) of the Electron Density at the Bond, Ring, and Cage Critical Points (CP) Originated upon Formation of the C−H···π Complexes

compound	CP	ρ	$\nabla^2\rho$	λ_1	λ_2	λ_3
CH_4	(3,−1)	0.0049	0.0169	−0.0028	−0.0001	0.0197
	(3,+1)	0.0048	0.0169	−0.0028	0.0001	0.0196
	(3,+3)	0.0043	0.0180	0.0028	0.0028	0.0125
$HCCl_3$	(3,−1)	0.0102	0.0357	−0.0075	−0.0004	0.0435
	(3,+1)	0.0101	0.0358	−0.0075	0.0004	0.0429
	(3,+3)	0.0084	0.0383	0.0090	0.0090	0.0202
C_6H_6	(3,−1)	0.0077	0.0271	−0.0051	−0.0002	0.0325
	(3,+1)	0.0077	0.0272	−0.0052	0.0002	0.0321
	(3,+3)	0.0065	0.0290	0.0059	0.0059	0.0172
HCCH	(3,−1)	0.0075	0.0266	−0.0050	−0.0002	0.0138
	(3,+1)	0.0074	0.0265	−0.0049	0.0002	0.0312
	(3,+3)	0.0064	0.0281	0.0055	0.0055	0.0171
HCN	(3,−1)	0.0086	0.0302	−0.0059	−0.0003	0.0363
	(3,+1)	0.0085	0.0302	−0.0059	0.0002	0.0359
	(3,+3)	0.0072	0.0320	0.0067	0.0067	0.0185
HF	(3,−1)	0.0083	0.0319	−0.0059	−0.0002	0.0381
	(3,+1)	0.0083	0.0319	−0.0059	0.0002	0.0377
	(3,+3)	0.0072	0.0321	0.0063	0.0063	0.0194
$HCCl_3$[a]	(3,−1)	0.0108	0.0365	−0.0088	−0.0016	0.0470
	(3,+1)	0.0089	0.0341	−0.0061	0.0011	0.0391
	(3,+3)	0.0078	0.0379	0.0085	0.0092	0.0202

[a] Complex of chloroform with fluorobenzene.

point and a cage critical point are also found for the complex of benzene with methane, they exhibit an arrangement similar to that found for the complex of chloroform with fluorobenzene. Again, these topologies satisfy the Poincaré−Hopf relationship. Thus, even though the energy difference between the C_s geometries and those having the C−H (F−H) group pointing toward the center of the ring is very small (vide supra), marked changes occur in the topology of the electron density.

(2) Charge Density at the Bond Critical Point. According to previous studies, the electron density at the bond critical point formed in hydrogen bonding varies typically in the range 0.002−0.034 atomic units (au), these values being sensibly lower than those found for (3,−1) critical points associated with covalent bonds. Table 2 reports the values of the electron density at the (3,−1), (3,+1), and (3,+3) critical points formed upon complexation with benzene.[22] The electron density at the bond critical points, which varies from ∼0.004 au in CH_4 to near 0.011 au in $CHCl_3$, fits within the expected range of values for similar interactions.[8c,9b]

Comparison of the density values at the (3,−1) critical points given in Table 2 with the corresponding interaction energies of the benzene complexes (Table 1) shows the existence a linear relationship (see Figure 2), as noted in the correlation coefficient ($r = 0.91$) of the regression equation $E = 2.716 - 6.036\ 10^2\rho$ (the energy is given in kcal/mol and the density in au). Analogous findings have been observed between the density at the (3,−1) critical point and the interaction energy in a variety of complexes.[15] Because all the complexes exhibit the same topological pattern, such a comparison can be performed considering the density at the (3,+1) and (3,+3) critical points. In particular, the following relationship holds for the density at the cage critical points: $E = 3.165 - 7.797\ 10^2\rho$ ($r = 0.92$), which agrees with similar findings recently reported for cation-π complexes.[7e] These relationships allow us to generalize the concept of bond order reported for other kinds of related interactions.[15]

(3) Laplacian of the Charge Density. It has been shown that the value of $\nabla^2\rho$ for the (3,−1) critical point in H bonds, and more generally for closed-shell interactions such as ionic bonds and van der Waals complexes, is positive. This feature is found

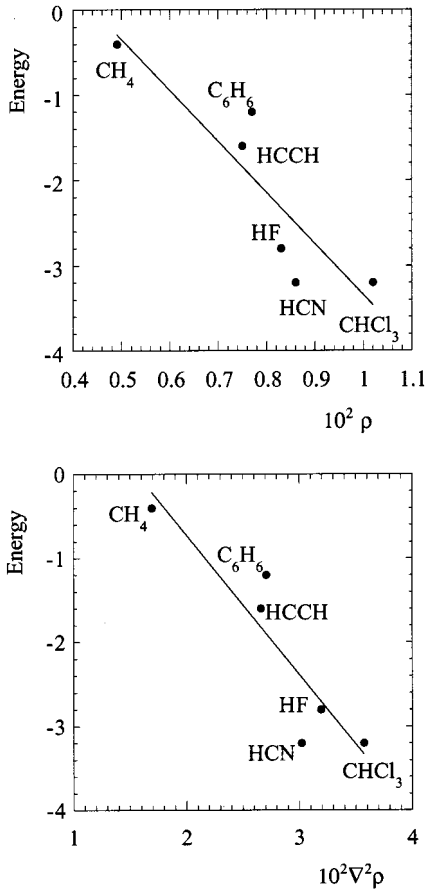

Figure 2. Representation of the variation in the BSSE-corrected interaction energy (kcal/mol) of the C−H···benzene complexes and the electron density (top) at the bond critical point and its laplacian (bottom).

in all the complexes (Table 2) and the values for the bond critical points, which are between 0.016 and 0.037 au, are similar to the range of values for typical H-bonded interactions, which can vary from 0.014 to 0.139 au.[8c] The positive value of the laplacian indicates a depletion of electron density from the interatomic surface toward the interacting nuclei, as noted in the positive value of λ_3, which is much larger than the other two eigenvalues. Another feature of the laplacian is the large magnitude of the ellipticity, which is defined as $\lambda_1/\lambda_2 - 1$, because it can be as large as 40 for the (3,−1) critical point formed upon complexation. This feature is an indication of structural instability, as it is also revealed by the closeness between bond and ring critical points.

Following the trends just mentioned for the electron density at the bond critical point, there is a clear relationship between the BSSE (basis set superposition error)-corrected interaction energy of the benzene complexes and the laplacian of the electron density, as can be stated from inspection of Figure 2. The regression equations for the bond and cage critical points are $E = 2.649 - 1.668\ 10^2\nabla^2\rho$ ($r = 0.92$) and $E = 2.608 - 1.569\ 10^2\nabla^2\rho$ ($r = 0.92$), respectively.

(4) Mutual Penetration of Hydrogen and Acceptor Atoms. The mutual penetration can be determined by comparison of the nonbonded radii (r^0) of both hydrogen and acceptor atoms with the corresponding bonded radii (r). The nonbonded radius was estimated as the distance from the nucleus to a given charge density contour (usually taken to be 0.001 au) in the direction of the H bond, whereas the bonded radius is determined from the distance of the nucleus to the bond critical point formed

TABLE 3: Nonbonded (r^0) and Bonded (r) Radii (au) of the Hydrogen and Carbon Atom for the Series of Benzene Complexes

compound	r^0_H	r_H	Δr_H [a]	r^0_C	r_C	Δr_C [a]	$\Delta r_H + \Delta r_C$
CH_4	2.59	2.24	0.35	3.95	3.41	0.54	0.89
$HCCl_3$	2.52	1.89	0.63	4.02	3.00	1.02	1.65
C_6H_6	2.58	2.04	0.54	3.97	3.14	0.83	1.37
HCCH	2.44	1.97	0.47	4.00	3.18	0.82	1.29
HCN	2.40	1.89	0.51	4.00	3.10	0.90	1.41
HF	2.12	1.73	0.39	4.03	3.11	0.92	1.31
$HCCl_3$ [b]	2.52	1.86	0.66	3.98	2.97	1.01	1.67

[a] $r^0 - r$. [b] Complex of chloroform with fluorobenzene.

TABLE 4: Integrated Atomic Properties[a] of the H Bond Hydrogen Atom in the Isolated Monomer and In the Complex, and the Change (Δ) of the Corresponding Property Arising Upon Complexation

compound	monomer	complex	Δ
	net charge		
CH_4	−0.027	−0.003	0.024
$HCCl_3$	0.097	0.128	0.031
C_6H_6	−0.008	0.018	0.026
HCCH	0.125	0.149	0.024
HCN	0.182	0.209	0.027
HF	0.713	0.716	0.003
$HCCl_3$ [b]	0.097	0.133	0.036
	energy		
CH_4	−0.6395	−0.6339	0.0056
$HCCl_3$	−0.6117	−0.6021	0.0096
C_6H_6	−0.6374	−0.6340	0.0034
HCCH	−0.5730	−0.5643	0.0087
HCN	−0.5466	−0.5362	0.0104
HF	−0.2919	−0.2879	0.0040
$HCCl_3$ [b]	−0.6117	−0.5950	0.0167
	first moment		
CH_4	0.134	0.110	−0.024
$HCCl_3$	0.132	0.107	−0.025
C_6H_6	0.128	0.097	−0.031
HCCH	0.114	0.096	−0.018
HCN	0.110	0.094	−0.016
HF	0.120	0.114	−0.006
$HCCl_3$ [b]	0.132	0.094	−0.038
	volume		
CH_4	51.59	48.05	−3.54
$HCCl_3$	41.72	28.97	−12.75
C_6H_6	50.27	40.77	−9.50
HCCH	42.89	36.43	−6.46
HCN	40.16	31.27	−8.89
HF	14.24	9.82	−4.42
$HCCl_3$ [b]	41.72	29.70	−12.02

[a] All values in atomic units. [b] Complex of chloroform with fluorobenzene.

upon complexation. The penetration is then defined as the difference between the nonbonded and bonded radius ($\Delta r = r^0 - r$). Table 3 shows the corresponding results, which indicate that in all cases the penetrations are positive and that the carbon atoms of the benzene ring are more penetrated that the hydrogen atom, in agreement with previous studies for related systems.[14c,d]

(5) Increase of Net Charge of the Hydrogen Atom. Another necessary condition for the formation of a H bond is the loss of charge of the hydrogen atom. The values of the net charge for the hydrogen atom in the isolated monomer and in the dimer, as well as their difference, are shown in Table 4. The results indicate that the hydrogen is descreened upon formation of the complex. The magnitude of this effect is between 0.022 and 0.036 units of electron for all the complexes but the dimer benzene···HF, where the net charge of the hydrogen atom increases only 0.003 units of electron upon binding. This particular behavior can be explained from the large descreening of the hydrogen in the isolated HF that is due to the strong electron-withdrawing nature of the fluorine atom. In all cases, there is a charge transfer from the aromatic ring to the proton donor molecule, which varies from only 0.004 units of electron for CH_4 to ∼0.025 units of electron for the polar molecules $CHCl_3$, HCN, and HF.

(6) Energetic Destabilization of the Hydrogen Atom. Another feature of H bond is the energetic destabilization of the hydrogen atom, which can be determined from the difference in atomic energies of the hydrogen in the isolated monomer and in the dimer. The results reported in Table 4 indicate that this quantity is positive in all cases, ranging from 0.0034 to 0.0104 au, which agrees with the destabilization observed in other H bond interactions.[8c,9b,14c,d]

(7) Decrease of Dipolar Polarization of the Hydrogen Atom. In addition to the preceding integrated properties, the first moment of the hydrogen atom must decrease upon formation of a H bond. The results in Table 4 show that complexation with benzene (and fluorobenzene) leads to a reduction in the first moment, which decreases between 0.006 (HF) and 0.031 ($CHCl_3$) au. Again, this range of variation compares with the changes observed in a variety of H bond complexes.[8c,9b]

(8) Decrease of the Atomic Volume of the Hydrogen Atom. The last criterion for the existence of a H bond is the decrease in the atomic volume of the hydrogen atom. The corresponding values for the isolated monomer and for the dimer are collected in Table 4. Inspection of the results indicate that the volume of the hydrogen atom is reduced by 3−13 au with regard to the volume in the isolated monomer. The change experienced by the hydrogen atom is sensibly larger than the variations observed in the rest of atoms within the molecule (data not shown), leading to a net reduction of the molecular volume in all the cases.

The preceding results indicate that the hydrogen atom involved in H-bonding exhibits analogous topological features of the electron density and similar changes in the integrated atomic properties in all cases. This common pattern consists of the appearance of a bond path linking the hydrogen atom to each carbon atom in the benzene ring and the corresponding bond critical point. The electron density at the (3,−1) critical point and its laplacian, which is positive as expected for a closed-shell interaction, fit within the expected range for H bond interactions. Finally, inspection of the integrated properties reveal a loss of electron density, which is accompanied by a reduction in the atomic volume, an energy destabilization of the atom, and a decrease in the atomic polarization. Therefore, as far as the criteria defining an H bond interaction are concerned, there is no relevant difference in the properties associated with the hydrogen atom for the series of compounds examined here, even though the results in Table 1 indicate that there is a fundamental division between complexes exhibiting features of conventional H bond or anti-H bond behavior. This result suggests that the phenomenon of the anti-H bond stems from the electron density redistribution in the C−H bond induced upon complexation. In an attempt to examine this assumption, we have determined the properties of the (3,−1) critical point associated with the C−H bond in the complex and in the isolated monomers.

Table 5 shows the distance from the bond critical point (BCP) to the carbon and hydrogen nuclei in the isolated monomer and in the complex. The results indicate that, as a result of complexation, the distance from the (3,−1) critical point to the carbon nucleus increases and the separation of the bond critical point to the hydrogen nucleus decreases. The magnitude of the

TABLE 5: Distance (au) of the (3,−1) Bond Critical Point (BCP) Associated with the C−H Bond to the Carbon and Hydrogen Nuclei in the Isolated Monomer and in the Complex

	BCP−carbon			BCP−hydrogen			
compound	m	d	Δ^a	m	d	Δ^a	net effect
CH_4	1.2735	1.2825	0.0090	0.7779	0.7670	−0.0109	−0.0019
$HCCl_3$	1.3418	1.3599	0.0181	0.7045	0.6822	−0.0283	−0.0042
C_6H_6	1.2783	1.2884	0.0101	0.7678	0.7512	−0.0166	−0.0065
HCCH	1.2927	1.3108	0.0181	0.7150	0.6985	−0.0165	0.0016
HCN	1.3206	1.3426	0.0220	0.6925	0.6731	−0.0194	0.0026
HF	1.4411	1.4507	0.0053	0.2996	0.2953	−0.0043	0.0053
$HCCl_3$[b]	1.3418	1.3607	0.0189	0.7045	0.6806	−0.0239	−0.0050

[a] Difference (dimer−monomer). [b] Complex of chloroform with fluorobenzene.

TABLE 6: Topological Properties of the Electron Density at (3,−1) Critical Point of the C−H Bond in the Isolated Monomer (m) and in the Complex (d)

molecule	form	ρ	$\nabla^2\rho$	λ_1	λ_2	λ_3
CH_4	m	0.2803	−0.9908	−0.7181	−0.7181	0.4455
	d	0.2824	−1.0118	−0.7307	−0.7307	0.4496
$HCCl_3$	m	0.3028	−1.2214	−0.8586	−0.8586	0.4959
	d	0.3062	−1.2762	−0.8832	−0.8832	0.4903
C_6H_6	m	0.2853	−1.0399	−0.7516	−0.7392	0.4509
	d	0.2899	−1.0821	−0.7753	−0.7633	0.4564
HCCH	m	0.2918	−1.1637	−0.7921	−0.7921	0.4205
	d	0.2930	−1.1939	−0.8077	−0.8077	0.4215
HCN	m	0.2914	−1.2067	−0.8148	−0.8148	0.4229
	d	0.2917	−1.2407	−0.8298	−0.8298	0.4189
HF	m	0.3715	−2.6333	−2.3254	−2.3254	2.0175
	d	0.3658	−2.6611	−2.3238	−2.3238	1.9866
$HCCl_3$[a]	m	0.3028	−1.2214	−0.8586	−0.8586	0.4959
	d	0.3164	−1.3984	−0.9271	−0.9269	0.4557

[a] Complex of chloroform with fluorobenzene.

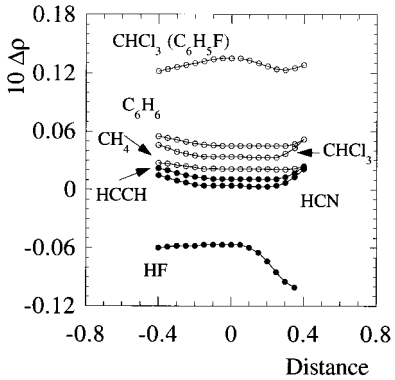

Figure 3. Profiles of electron density difference (au) computed as the difference between the electron density of the monomer in the dimer and that of the isolated monomer along the bond path associated with the C−H bond as the distance (au) from the (3,−1) critical point is enlarged. The origin of distance is located at the bond critical point.

two effects is rather comparable: whereas the distance BCP−carbon is elongated by 0.005−0.022 au, the distance BCP−hydrogen is reduced by 0.004−0.028 au. It is worth noting, however, that the relative magnitude of these two effects is different in those compounds exhibiting anti-H bond behavior with regard to those forming normal H bond complexes. Thus, the shortening of the distance BCP−hydrogen in CH_4, $CHCl_3$, and C_6H_6 is 0.0019−0.0065 larger than the elongation of the carbon nucleus from the BCP, leading to a net reduction in the bond length, as stated in Table 1. Contrarily, the reverse trend is observed in HCCH, HCN, and HF, the net effect being the increase in the bond length (see Table 1).

The values of the electron density at the (3,−1) critical point and its associated properties are given in Table 6. The electron density is sensibly larger than the value obtained for the intermolecular (3,−1) critical point (see Table 2). Indeed, in contrast to the positive values of the laplacian reported in Table 2, the laplacian is negative, which indicates that there is a concentration of charge density between the bonded atoms, as expected for a covalent interaction. In all cases, the laplacian becomes more negative upon formation of the complex, the magnitude of this effect ranging from −0.021 (CH_4) to −0.055 ($CHCl_3$; −0.177 for the complex with fluorobenzene) au. This change in the laplacian arises mainly from an increase (in absolute value) of the curvatures in the directions normal to the bond path (λ_1, λ_2). The only exception is the complex of benzene with HF because the main change is associated with the curvature along the bond path (λ_3), which decreases upon formation of the complex. This effect is also observed in the two other polar compounds considered here, $CHCl_3$ and HCN, whereas the reverse trend is found for CH_4, C_6H_6, and HCCH.

The results in Table 6 show that the electron density at the bond critical point is enlarged upon complexation in all cases, but for HF, where the electron density at the (3,−1) critical point of the H−F bond is 0.0057 au lower in the complex than in the isolated monomer. This effect is also found in the C_s optimized structures of the benzene complexes with methane and hydrogen fluoride: whereas the electron density at the bond critical point of the C−H bond in the complex with methane is enlarged 0.0021 au, that of the F−H bond in the complex with hydrogen fluoride decreases by 0.0064 au. Such a change in the electron density at the bond critical point extends over a wide region around the bond critical point, as can be seen in Figure 3, which shows the profiles of electron density difference ($\rho_{C-H;complex} - \rho_{C-H;isolated\ monomer}$) along the C−H bond as the distance from the bond critical point is increased.

More interestingly, inspection of Figure 3 reveals that the electron density difference profiles for the different compounds are roughly parallel in the interval ±0.4 au from the bond critical point. The largest changes in electron density are found for $CHCl_3$ (complexed to fluorobenzene), where the electron density at the bond critical point is enlarged by >0.01 au, and for HF, where it is reduced by near 0.06 au. Moreover, there is a gradual variation in the electron density for the benzene complexes with the different carbon proton donors, the change in electron density at the (3,−1) critical point being reduced from 0.0046 au for C_6H_6 to only 0.0003 au for HCN (see Table 6).

Because the electron density at the bond critical point provides a measure of the bond order,[7e,13,15] one can reasonably assume that the change in electron density at the bond critical point induced upon complexation gives a measure of the variation in the strength of the bond. Accordingly, such a change can be expected to reflect at least qualitatively the shifts in bond length and stretching frequency for a series of related chemical systems. This can be verified for the benzene complexes with carbon proton donors in Figure 4, which shows significant correlations between the change in electron density at the (3,−1) critical

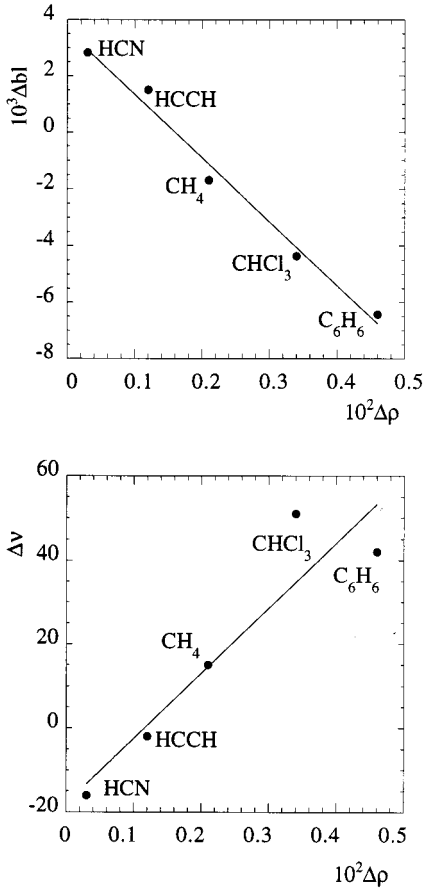

Figure 4. Representation of the shift in bond length (au; top) and stretching frequency (cm^{-1}; bottom) with the change in electron density (au) at the bond critical point of the C−H bond for the benzene complexes with the different carbon proton donors.

point of the C−H bond and the corresponding variations in bond lengths ($r = 0.99$) and stretching frequencies ($r = 0.94$).

The topological analysis already discussed shows no relevant difference for the series of benzene complexes as far as Popelier's criteria for H bonding are concerned. These criteria are focused on the changes in electron density occurring between the hydrogen atom of the donor molecule and the acceptor atom of the interacting partner, as well as on the integrated properties of the hydrogen atom. However, these criteria do not suffice to distinguish between a normal H bond and an anti-H bond complex, which are determined by subtle changes in the electron density of the covalent bond donating the hydrogen atom. These changes are clearly manifested in the increase/decrease of electron density observed in the complexes of fluorobenzene with chloroform and of benzene with hydrogen fluoride, respectively, but even for the related C−H···π benzene complexes a good correlation exists between the change in electron density with the shifts in bond length and vibrational frequency.

Conclusion

The results reported in this study provide a complementary interpretation of the anti-H bonding, which is phenomenologically manifested in the series of benzene complexes examined here as a shortening of the C−H bond length and a blue shift of its stretching frequency. As noted previously by Hobza,[11] such a phenomenon arises from the dominant stabilizing role of the dispersion forces. The results presented here allow us to suggest that the topological criteria proposed by Popelier are not sufficient to characterize such different phenomena as H bonding and anti-H bonding, as demonstrated by the red and blue shift of the respective X−H stretching frequencies. AIM facilitates discrimination between structurally different motifs with and without participation of hydrogen between two heavy atoms. Thus, H bonded criteria based on AIM are satisfied for standard X−H···Y H bonding, nonconventional C−H···O H bonding, and dihydrogen D−H···H−E bonding, and provide a basis to distinguish these interactions from van der Waals interactions of the X···Y type. To differentiate between H bonding and anti-H bonding, our results suggests that it is necessary to supplement those criteria with information on the changes in the electron density of the donor X−H bond occurring upon complexation.

Acknowledgment. We thank Prof. R. W. F. Bader for sending us a copy of PROAIM computer program. This work was supported by the DGICYT under projects PB97-0908 and PB96-1005, and by the Centre de Supercomputació de Catalunya (CESCA; Molecular Recognition Project).

Supporting Information Available: Table listing coordinates and energies are available. This information is available free of charge via the Internet at http://pubs.acs.org.

References and Notes

(1) (a) *Molecular Interactions. From van der Waals to Strongly Bound Complexes*; Scheiner, S., Ed.; Wiley: Chichester, 1997. (b) Adams, H.; Carver, F. J.; Hunter, C. A.; Osborne, N. J. *Chem. Commun.* **1996**, 2529. (c) Adams, H.; Harris, K. D. M.; Hembury, G. A.; Hunter, C. A.; Ivingstone, D.; McCabe, J. F. *Chem. Commun.* **1996**, 2531. (d) Kim, E.; Paliwal, S.; Wilcox, C. S. *J. Am. Chem. Soc.* **1998**, *120*, 11192. (e) Samanta, U.; Chakrabarti, P.; Chandrasekhar, J. *J. Phys. Chem. A* **1998**, *102*, 8964.

(2) Jeffrey, G. A.; Saenger, W. *Hydrogen Bonding in Biological Structures*; Springer: Berlin, 1991.

(3) Karpfen, A.; Yanovitskii, O. *J. Mol. Struct. (THEOCHEM)* **1994**, *314*, 211.

(4) (a) Suhai, S. *J. Chem. Phys.* **1994**, *101*, 9766. (b) Ojamäe, L.; Hermansson, K. *J. Phys. Chem.* **194**, *98*, 4271. (c) Contador, J. C.; Aguilar, M. A.; Sánchez, M. L.; Olivares del Valle, F. J. *J. Mol. Struct. (THEOCHEM)* **1994**, *314*, 229. (d) Estrin, D. A.; Paglieri, L.; Corongiu, G.; Clementi, E. *J. Phys. Chem.* **1996**, *100*, 8701. (e) Chen, W.; Gordon, M. *J. Phys. Chem.* **1996**, *100*, 14136. (f) Cruzan, J. D.; Braly, L. B.; Liu, K.; Brown, M. G.; Loeser, J. G.; Saykally, R. J. *Science* **1996**, *271*, 59. (g) Liu, K.; Brown, M. G.; Cruzan, J. D.; Saykally, R. J. *Science* **1996**, *271*, 62. (i) Gresh, N. *J. Phys. Chem. A* **1997**, *101*, 8680.

(5) (a) Guo, H.; Karplus, M. *J. Phys. Chem.* **1994**, *98*, 7104. (b) Gung, B.; Zhu, Z. *Tetrahedron Lett.* **1996**, *37*, 2189. (c) Zhbankov, R. G. *J. Mol. Struct.* ***1992***, *270*, 523. (d) Jorgensen, W. L.; Damm, W.; Frontera, A.; Lamb, M. L. In *Physical Supramolecular Chemistry*; Echegoyen, L., Kaifer, A. E., Eds.; Kluwer: Amsterdam, 1996; pp 115−126. (e) Luque, F. J.; López, J. M.; López de Paz, M.; Vicent, C.; Orozco, M. *J. Phys. Chem. A* **1998**, *102*, 6690.

(6) (a) Cooney, M.; Czernuszewicz, G.; Postel, E. H.; Flint, S. J.; Hogan, M. E. *Science* **1988**, *241*, 456. (b) Grigoriev, M.; Praseuth, D.; Guieysee, A. L.; Robin, P.; Thuong, N. T.; Harel-Bellan, A. *Proc. Natl. Acad. Sci., U.S.A.* **1993**, *90*, 3501 (c) Sun, J. S.; Garestier, T.; Hélène, C. *Curr. Opin. Struct. Biol.* **1996**, *6*, 327.

(7) (a) Tang, T. H.; Hu, W. J.; Yan, D.; Y.; Cui, Y. P. *J. Mol. Struct. (THEOCHEM)* **1990**, *207*, 319. (b) Atwood, J. L.; Hamada, F.; Robinson, K. D.; Orr, G. W.; Vincent, R. L. *Nature* **1991**, *349*, 683. (c) Suzuki, S.; Green, P. G.; Bumgarner, R. E.; Dasgupta, S.; Goddard, W. A., III.; Blake, G. A. *Science* **1992**, *257*, 942. (d) Pribble, R. N.; Garret, A. W.; Haber, K.; Zwier, T. S. J. Chem. Phys. **1995**, *103*, 531. (e) Cubero, E.; Orozco, M.; Luque, F. J. *J. Phys. Chem. A* **1999**, *103*, 315.

(8) (a) Desiraju, G. R. *Acc. Chem. Res.* **1991**, *24*, 290. (b) Desiraju, G.; Kashino, S.; Coombs, M. M.; Glisker, J. *Acta Crystallogr.* **1993**, *B49*, 880. (c) Kock, U.; Popelier, P. L. A. *J. Phys. Chem.* **1995**, *99*, 9747. (d) Alkorta, I.; Campillo, N.; Rozas, I.; Elguero, J. *J. Org. Chem.* **1998**, *63*, 7759.

(9) (a) Richardson, T. B.; de Gala, S.; Crabtree, R. H.; Siegbahn, P. E. M. *J. Am. Chem. Soc.* **1995**, *117*, 12875. (b) Popelier, P. L. A. *J. Phys. Chem. A* **1998**, *102*, 1873.

(10) (a) Park, S.; Ramachandran, R.; Lough, A. J.; Morris, R. H. *J. Chem. Soc., Chem. Commun.* **1994**, 2201. (b) Peris, E.; Lee, J. C.; Rambo, J. R.; Eisenstein, O.; Crabtree, R. H. *J. Am. Chem. Soc.* **1995**, *117*, 3485. (c) Wessel, J.; Lee, J. C.; Peris, E.; Yap, G. P. A.; Fortin, J. B.; Ricci, J. S.;

Sini, G.; Albinati, A.; Koetzle, T. F.; Eisenstein, O.; Rheingold, A. L.; Crabtree, R. H. *Angew. Chem., Int. Ed. Engl*. **1995**, *34*, 2507. (d) Crabtree, R. H.; Siegbahn, P. E. M.; Eisenstein, O.; Rheingold, A.; Koetzle, T. F. *Acc. Chem. Res.* **1996**, *29*, 348.

(11) Hobza, P.; Spirko, V.; Selzle, H. L.; Schlag, E. W. *J. Phys. Chem. A* **1998**, *102*, 2501.

(12) Hobza, P.; Spirko, V.; Havlas, Z.; Buchhold, K.; Reimann, B.; Barth, H. D.; Brutschy, B. *Chem. Phys. Lett.* **1999**, *299*, 180.

(13) (a) Bader, R. F. W. *Atoms in Molecules. A Quantum Theory;* Oxford University Press: Oxford. 1990. (b) Bader, R. F. W. *Chem. Rev.* **1991**, *91*, 893. (c) Bader, R. F. W. *J. Phys. Chem. A* **1998**, *102*, 7314.

(14) (a) Carroll, M. T.; Chang, C.; Bader, R. F. W. *Mol. Phys*. **1988**, *65*, 695. (b) Destro, R.; Bianchi, R.; Gatti, C.; Merati, F. *Chem. Phys. Lett.* **1991**, *186*, 47. (b) Gonzalez, L.; Mo, O.; Yañez, M.; Elguero, J. *J. Mol. Struct. (THEOCHEM)* **1996**, *371*, 1. (c) Rozas, I.; Alkorta, I.; Elguero, J. *J. Phys. Chem. A* **1997**, *101*, 9457. (d) Alkorta, I.; Rozas, I.; Elguero, J. *Theor. Chem. Acc.* **1998**, *99*, 116. (e) Novoa, J. J.; Lafuente, P.; Mota, F. *Chem. Phys. Lett.*. **1998**, *290*, 519. (f) Luisi, B.; Orozco, M.; Sponer, J.; Luque, F. J.; Cole, J. C.; Shakked, J. Z. *J. Mol. Biol.* **1998**, *279*, 1125.

(15) (a) Boyd, R. J.; Choi, S. C. *Chem. Phys. Lett.*. **1985**, *120*, 80. (b) *ibidem.* **1986**, *129*, 62. (c) Bader, R. F. W.; Tang, T. H.; Tal, Y.; Biegler-König, F. *J. Am. Chem. Soc.* **1982**, *104*, 946. (d) Alkorta, I.; Elguero, J. *J. Phys. Chem.* **1996**, *100*, 19367. (e) Mallinson, P. R.; Wozniak, K.; Smith, G. T.; McCormack, K. L. *J. Am. Chem. Soc.* **1997**, *119*, 11502. (f) Roversi, P.; Barzaghi, M.; Merati, F.; Destro, R. *Can. J. Chem.* **1996**, *74*, 4, 1145. (g) Mo, O.; Yáñez, M.; Elguero, J. *J. Chem. Phys.* **1992**, *97*, 6628. (h) Alkorta, I.; Campillo, N.; Rozas, I.; Elguero, J. *J. Org. Chem.* **1998**, *63*, 7759. (i) Alkorta, I.; Rozas, I.; Elguero, J. *Struct. Chem.* **1998**, *9*, 243.

(16) Møller, C.; Plesset, M. S. *Phys. Rev.* **1934**, *46*, 618.

(17) Hariharan, P. C.; Pople, J. A. *Theor. Chim. Acta* **1973**, *28*, 213.

(18) Boys, S. F.; Bernardi, F. *Mol. Phys.* **1970**, *19*, 553.

(19) Gaussian 94 (Rev. A.1). Frisch, M. J.; Trucks, G. W.; Schlegel, H. B.; Gill, P. M. W.; Johnson, B. G.; Robb, M. A.; Cheeseman, J. R.; Keith, T. A.; Petersson, G. A.; Montgomery, G. A.; Raghavachari, K.; Al-Laham, M. A.; Zakrzewskim V. G.; Ortiz, J. V.; Foresman, J. B.; Cioslowski, J.; Stefanov, B. B.; Nanayakkara, A.; Challacombe, M.; Peng, C. Y.; Ayala, P. Y.; Chen, W.; Wong, M. W.; Andres, J. L.; Replogle, E. S.; Gomperts, R.; Martin, R. L.; Fox, D. J.; Binkley, J. S.; Defrees, D. J.; Baker, J.; Stewart, J. J. P.; Head-Gordon, M.; Gonzalez, C.; Pople, J. A. Gaussian. Inc.; Pittsburgh, PA, 1995.

(20) Biegler-König, F.; Bader, R. F. W.; Tang, T. H. *J. Comput. Chem.* **1982**, *3*, 317.

(21) Let us note that the cage critical point is surrounded by two ring critical points: one corresponds to the ring critical point formed near C1, the carbon atom bearing the fluorine atom, and the other is the ring critical point of the benzene ring.

(22) The values of the density and the laplacian at the bond critical points of the C_s minimum energy structures are (in atomic units) $\rho = 0.0052, \nabla^2\rho = 0.0171$ and $\rho = 0.0110, \nabla^2\rho = 0.0349$ for the benzene complexes with methane and hydrogen fluoride, respectively.